

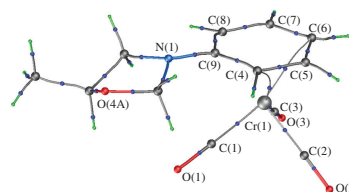
Experimental, experimental–theoretical and theoretical estimates of intermolecular interaction energies in η^6 -[(5-methyl-1,3-oxazolidin-3-yl)benzene]tricarbonylchromium(0)

Georgy K. Fukin* and Anton V. Cherkasov

G. A. Razuvaev Institute of Organometallic Chemistry, Russian Academy of Sciences, 603137 Nizhny Novgorod, Russian Federation. E-mail: gera@iomc.ras.ru

DOI: 10.1016/j.mencom.2021.03.012

The electron density distribution based on a whole-molecule aspherical scattering factor (molecular invariom) and an asymmetric unit-cell aspherical scattering factor (crystal invariom) allows us to analyze both intramolecular and intermolecular interactions in a crystal with sufficient accuracy.



Keywords: high-resolution X-ray diffraction, charge density, periodical DFT calculation, (η^6 -arene)tricarbonylchromium.

Difficulties in obtaining highly reflective crystals to study experimental electron density (ED) topology have led to the development of the concept of invarioms^{1,2} (aspherical atomic scattering factors). This concept successfully describes the topological characteristics of covalent bonds and intermolecular interactions in organic molecular and inorganic crystals and in salts.^{3–13} By definition, invarioms do not contain information about crystal package effects. The next step in the development of invarioms was a molecular invariom (whole-molecule aspherical scattering factor). In contrast to organic and inorganic compounds, organometallic and coordination compounds have relatively soft coordination spheres. In other words, the same metal atoms with similar coordination environments in different complexes can have different geometric characteristics of the coordination sphere. As a result, the invarioms of the same metal atom and the atoms of its coordination environment are different in each particular case. Therefore, the application of the molecular invariom to coordination and organometallic compounds allows one to more correctly model the ED topology especially in the coordination sphere of a metal atom. The molecular invarioms were used not only for the identification of metal atoms in coordination compounds,^{14,15} the analysis of agostic interactions in the $[\text{Cp}_2\text{FeH}](\text{PF}_6)$ ¹⁶ complex, and the estimation of *d*-orbital populations¹⁷ but also for the analysis of ED topological characteristics in coordination spheres of metal atoms.^{18–20} Note that differences in the ED $[\rho(\mathbf{r})]$ and its laplacian $[\nabla^2\rho(\mathbf{r})]$ at the critical points (3,–1) [CP (3,–1)] obtained experimentally and experimentally–theoretically (molecular invarioms) do not exceed the transferability index $[\rho(\mathbf{r}) = 0.1 \text{ e } \text{Å}^{-3} (0.015 \text{ a.u.}), \nabla^2\rho(\mathbf{r}) = 3–4 \text{ e } \text{Å}^{-5} (0.12–0.17 \text{ a.u.})]$ for these quantities.²¹ As noted above, invarioms and molecular invarioms do not contain information on intermolecular interactions in crystals; nevertheless, they are used to evaluate them. For this reason, we propose to use an asymmetric unit-cell aspherical scattering factor (crystal invariom) to evaluate the energy and topological characteristics of intermolecular interactions at CP (3,–1). Thus, the central point of this study is to compare the energies of intermolecular interactions based on the example of η^6 -[(5-

methyl-1,3-oxazolidin-3-yl)benzene]tricarbonylchromium(0). For this purpose, we carried out experimental (high-resolution X-ray diffraction study; $\mathbf{1}_{\text{exp}}$), experimental–theoretical (molecular and crystal invarioms; $\mathbf{1}_{\text{mol}}$ and $\mathbf{1}_{\text{cryst}}$), and theoretical (periodic DFT calculation of a crystal with geometry optimization by the Crystal 17 program²²; $\mathbf{1}_{\text{theor}}$) studies of the ED distribution. In addition, we obtained theoretically calculated structural amplitudes from the DFT calculation, which were used in multipole refinement $\mathbf{1}_{\text{theor}}$ (hereafter $\mathbf{1}_{\text{thmul}}$). The criterion for the presence of intermolecular interaction is CP (3,–1) between the atoms, and the energy is determined according to the Espinosa–Molins–Lecomte (EML) correlation.²³ Previously, such a method of estimating the intermolecular interaction energy showed its reliability.^{24–27}

The synthesis and structure of η^6 -[(5-methyl-1,3-oxazolidin-3-yl)benzene]tricarbonylchromium(0) ($\mathbf{1}_{\text{exp}}$) were described earlier.²⁸ Comparison of the experimental topological ED characteristics in the coordination sphere of the chromium atom ($\mathbf{1}_{\text{exp}}$)[†] with similar values obtained in $\mathbf{1}_{\text{mol}}$, $\mathbf{1}_{\text{cryst}}$, $\mathbf{1}_{\text{theor}}$, and

[†] The data were collected on a Bruker D8 Quest diffractometer for $\mathbf{1}_{\text{exp}}$ (graphite-monochromated MoK α radiation) at 100 K. The structure was solved by dual methods and refined on F^2 using the SHELXTL package.²⁹ All non-hydrogen atoms were refined anisotropically. All hydrogen atoms were placed in calculated positions and refined in the riding model. SADABS³⁰ was used to perform area-detector scaling and absorption corrections.

Crystal data for $\mathbf{1}_{\text{exp}}$. *M* = 299.24, orthorhombic, space group *Pna*2₁, *a* = 16.3105(5) Å, *b* = 7.4537(2) Å, *c* = 10.1614(3) Å, $\alpha = \beta = \gamma = 90^\circ$, *V* = 1235.36(6) Å³, *Z* = 4, *d*_{calc} = 1.609 mg m^{–3}, $\mu = 0.935 \text{ mm}^{-1}$, *F*(000) = 616. Intensities of 323977 reflections were measured ($\theta < 53.713^\circ$) and 15068 independent reflections [*R*_{int} = 0.0332] were used in further refinement. For $\mathbf{1}_{\text{exp}}$ the refinement converged to *wR*₂ = 0.0775 and goodness of fit *GOF* = 1.002 for all observed reflections [*R*₁ = 0.0297 was calculated against *F* for 14688 observed reflections with *I* > 2 σ (*I*)]. The residual electron densities (max/min) are 0.569 / –0.703 e Å^{–3} for $\mathbf{1}_{\text{exp}}$.

The multipole refinement was carried out within the Hansen–Coppens formalism³¹ using the MoPro program package.³² Before the refinement, C–H bond distances were normalized to the values obtained in neutron diffraction analyses.³³ The levels of the multipole expansion were

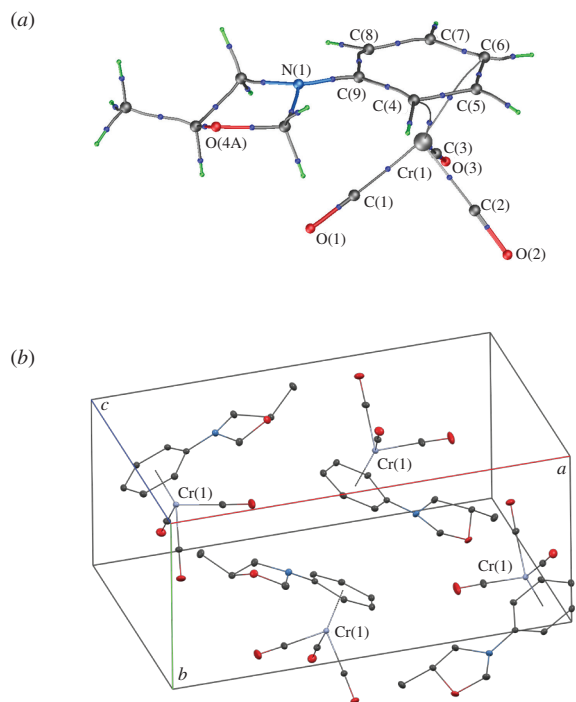


Figure 1 (a) Experimental molecular graph and (b) unit cell of complex $\mathbf{1}_{\text{exp}}$. The critical points CP(3,-1) are presented by blue points.

$\mathbf{1}_{\text{thmul}}$ showed that these differences do not exceed the transferability indices²¹ for $\rho(\mathbf{r})$ [$0.1 \text{ e } \text{\AA}^{-3}$ (0.015 a.u.)] and $\nabla^2\rho(\mathbf{r})$ [$3\text{--}4 \text{ e } \text{\AA}^{-5}$ (0.12–0.17 a.u.)] (Table S1, Online Supplementary Materials). However, all multipole models ($\mathbf{1}_{\text{exp}}$, $\mathbf{1}_{\text{mol}}$, $\mathbf{1}_{\text{cryst}}$, and $\mathbf{1}_{\text{thmul}}$) reproduce the $\nabla^2\rho(\mathbf{r})$ signs on the C≡O bonds in contrast to $\mathbf{1}_{\text{theor}}$ (Table S1). It should be noted that the DFT calculations of isolated (η^6 -arene)tricarbonylchromium molecules also did not reproduce the $\nabla^2\rho(\mathbf{r})$ signs on the C≡O bonds.^{19,36,37} As with related (η^6 -arene)tricarbonylchromium complexes,^{36–38} not all of the expected bond paths and CP(3,-1) are localized between the chromium atom and the arene ligand.

The unit cell of $\mathbf{1}_{\text{exp}}$ contains four molecules [Figure 1(b)]. Therefore, to compare the intermolecular interaction energies obtained using different methods ($\mathbf{1}_{\text{exp}}$, $\mathbf{1}_{\text{mol}}$, $\mathbf{1}_{\text{cryst}}$, $\mathbf{1}_{\text{thmul}}$ and $\mathbf{1}_{\text{theor}}$), we analyzed these interactions detected within one cell (Table 1) and compared them with the experimental data ($\mathbf{1}_{\text{exp}}$). The intermolecular interactions detected in $\mathbf{1}_{\text{mol}}$, $\mathbf{1}_{\text{cryst}}$, $\mathbf{1}_{\text{thmul}}$ and $\mathbf{1}_{\text{theor}}$ within the cell but not confirmed in $\mathbf{1}_{\text{exp}}$ are not given in Table 1. The total number of intermolecular contacts detected within the cell in $\mathbf{1}_{\text{theor}}$ is 21; 15, 18, 16 and 17 contacts were found in $\mathbf{1}_{\text{exp}}$, $\mathbf{1}_{\text{mol}}$, $\mathbf{1}_{\text{cryst}}$ and $\mathbf{1}_{\text{thmul}}$, respectively (Tables S2–S6, Figures S1–S3). Note that model $\mathbf{1}_{\text{thmul}}$, in contrast to $\mathbf{1}_{\text{theor}}$, finds approximately the same number of intermolecular interactions within the cell as $\mathbf{1}_{\text{mol}}$ and $\mathbf{1}_{\text{cryst}}$. This can be caused by different representations of the ED (multipole expansion for

hexadecapole for the chromium atom, octupole for all other non-hydrogen atoms, and one dipole for hydrogen atoms.

The refinement of compound $\mathbf{1}_{\text{exp}}$ ($\theta < 51.42^\circ$) was carried out against F and converged to $R = 0.0322$, $wR = 0.0281$, $\text{GOF} = 0.991$ for 13167 merged reflections with $I > 0.5\sigma(I)$. The ratio of the number of reflections to the number of refined parameters was >10 for $\mathbf{1}_{\text{exp}}$. All bonded pairs of atoms satisfy the Hirshfeld rigid-bond criteria.³⁴ The topology of experimental $\rho(\mathbf{r})$ function was analyzed using the WinXPRO program package.³⁵ The residual electron densities around chromium atoms were no greater than $\sim 0.5 \text{ e } \text{\AA}^{-3}$ for $\mathbf{1}_{\text{exp}}$.

CCDC 2039330 (for IAM refinement) and 2039331 (for multipole refinement) contain the supplementary crystallographic data for this paper. These data can be obtained free of charge from The Cambridge Crystallographic Data Centre via <http://www.ccdc.cam.ac.uk>.

$\mathbf{1}_{\text{mol}}$, $\mathbf{1}_{\text{cryst}}$ and $\mathbf{1}_{\text{thmul}}$ and MO-LCAO for $\mathbf{1}_{\text{theor}}$). Nevertheless, all approaches somewhat overestimate the number of intermolecular interactions in the unit cell compared to the experiment. In turn, the crystal invariom ($\mathbf{1}_{\text{cryst}}$) most accurately reproduces the total number of intermolecular interactions (16 interactions) in the unit cell of $\mathbf{1}_{\text{exp}}$ (15 interactions). According to Table 1, the molecular invariom ($\mathbf{1}_{\text{mol}}$) reproduces 13 interactions from 15 in $\mathbf{1}_{\text{exp}}$, while $\mathbf{1}_{\text{cryst}}$, $\mathbf{1}_{\text{thmul}}$ and $\mathbf{1}_{\text{theor}}$ find 12, 11 and 10 ones, respectively. A comparison of the intermolecular interaction energies (see Table 1) showed that the experimental–theoretical and theoretical methods systematically exceed the experimental values (except for $\mathbf{1}_{\text{thmul}}$). In $\mathbf{1}_{\text{thmul}}$, the numbers of overestimated and underestimated intermolecular interactions, as compared with the experimental energy values in $\mathbf{1}_{\text{exp}}$, were approximately the same. Surprisingly, with the exception of two intermolecular interactions [O(2)⋯H(12A) and O(3)⋯N(1)], the molecular invariom describes the experimental energy in $\mathbf{1}_{\text{exp}}$ more accurately than the crystal one. In other words, the crystal invariom, which takes into account packing effects in contrast to the molecular one, somewhat less accurately reproduces the energy values of intermolecular interactions in $\mathbf{1}_{\text{exp}}$. Moreover, the theory shows the greatest deviations from the experiment. The most significant differences for all approaches ($\mathbf{1}_{\text{mol}}$, $\mathbf{1}_{\text{cryst}}$, $\mathbf{1}_{\text{theor}}$, and $\mathbf{1}_{\text{thmul}}$) are observed in the O(3)⋯H(5A) and H(6A)⋯H(11A) interactions. The largest energy difference between other experimental–theoretical ($\mathbf{1}_{\text{mol}}$, $\mathbf{1}_{\text{cryst}}$) and theoretical ($\mathbf{1}_{\text{theor}}$, $\mathbf{1}_{\text{thmul}}$) intermolecular interactions does not exceed experimental values by 50 and 64%, respectively.

In order to increase the reliability of the study, we carried out crystal lattice energy estimations in two ways: (1) as the sum of energies of intermolecular pair interactions between the considered molecule and its neighbors and (2) as the difference between the molecule energy in the lattice and the energy of an optimized molecule in the superlattice (a difference approach^{39,40}). This approach is reliable for estimating sublimation enthalpies.²⁴ Table 2 shows lattice energies obtained for different models. The experimentally calculated lattice energy of $\mathbf{1}_{\text{exp}}$ is in good agreement with theoretical estimates obtained in $\mathbf{1}_{\text{theor}}$. It is fundamentally important that the theoretical estimation was carried out by two independent ways. In turn, $\mathbf{1}_{\text{mol}}$, $\mathbf{1}_{\text{cryst}}$ and $\mathbf{1}_{\text{thmul}}$ overestimate the experimental lattice energy in $\mathbf{1}_{\text{exp}}$ by $\sim 35\text{--}60\%$ despite the fact that they reproduce well the intermolecular interaction energy within a cell. Therefore, it is important to understand how such a difference in the lattice

Table 1 Experimental ($\mathbf{1}_{\text{exp}}$), experimental–theoretical ($\mathbf{1}_{\text{mol}}$, $\mathbf{1}_{\text{cryst}}$) and theoretical ($\mathbf{1}_{\text{theor}}$, $\mathbf{1}_{\text{thmul}}$) intermolecular interaction energies.

Contact	$E_{\text{int}} / \text{kcal mol}^{-1}$			
	$\mathbf{1}_{\text{exp}}$	$\mathbf{1}_{\text{mol}}$	$\mathbf{1}_{\text{cryst}}$	$\mathbf{1}_{\text{thmul}} / \mathbf{1}_{\text{theor}}$
O(1)⋯O(4)	0.35	0.41	0.43	0.31/–
O(1)⋯C(6)	0.73	–	–	–/–
O(1)⋯H(13C)	0.43	0.47	0.51	0.31/1.19
O(2)⋯H(7A)	1.32	1.59	1.74	1.57/1.82
O(2)⋯H(10B)	1.12	1.18	1.46	1.26/1.99
O(2)⋯H(12A)	0.60	0.62	0.62	0.63/0.82
O(2)⋯H(13A)	0.38	0.41	0.50	0.31/0.57
O(2)⋯H(13B)	0.68	0.74	0.84	0.63/0.86
O(3)⋯N(1)	0.70	0.63	0.63	0.63/–
O(3)⋯C(8)	0.73	0.60	–	–/0.53
O(3)⋯H(5A)	0.53	0.81	0.98	0.63/2.12
C(6)⋯H(13C)	0.78	0.90	0.91	0.63/–
C(13)⋯H(4A)	0.53	0.53	0.57	–/–
H(5A)⋯H(13B)	0.26	–	–	–/–
H(6A)⋯H(11A)	0.22	0.62	0.79	0.63/1.29

Table 2 Lattice energies.

Lattice energy	I_{exp}^a	I_{mol}^a	I_{cryst}^a	I_{thmul}^a	I_{theor}^a	I_{theor}^b
kcal mol ⁻¹	23.36	31.43	37.36	35.35	25.0	19.45

^a The sum of energies of intermolecular pair interactions. ^b The difference approach.

energies affects the accuracy of the estimate of the intermolecular interactions energy obtained experimentally–theoretically. Due to the fact that the molecular invariom more accurately reproduces the experimental energies of intermolecular interactions in the cell (see Table 1) and the experimental lattice energy (see Table 2) compared to the crystalline one, we analyzed all intermolecular contacts in I_{exp} and I_{mol} and found 32 and 40 intermolecular contacts in I_{exp} and I_{mol} , respectively. With few exceptions (two H···H and one O···H contacts), the molecular invariom overestimates the experimental values of intermolecular interactions by 3–20% and underestimates them by no more than 20%. Thus, the molecular invariom sufficiently accurately reproduces the experimental energies of intermolecular interactions. Consequently, a 35% difference in lattice energies obtained from experimental and experimental–theoretical data is not critical. Thus, the molecular invariom can be used not only for the analysis of electron density topology in the coordination sphere of a metal atom but also for a semi-quantitative estimation of the energy of intermolecular interactions. A similar situation is observed in I_{cryst} , except for a slightly higher overestimation of the intermolecular interaction energy. Thus, in the absence of experimental data on the lattice energy, a theoretical estimate based on quantum-chemical calculations should be used.^{39,40} The agreement in lattice energy values obtained experimentally–theoretically and theoretically can serve as an integral quality characteristic for the description of intermolecular interactions.

However, it remains unclear why the packing effect taken into account in the crystal invariom does not markedly improve the energy values of the intermolecular interactions compared to those based on the molecular one. It may be necessary to use diffuse orbitals for a more accurate reproduction of the crystal package effect when constructing a crystal invariom.

In conclusion, based on an example of η^6 -[(5-methyl-1,3-oxazolidin-3-yl)benzene]tricarbonylchromium(0), we found that the approach comprising a whole-molecule aspherical scattering factor (molecular invariom) and an asymmetric unit cell aspherical scattering factor (crystal invariom) can be used not only to study the ED topology in the coordination sphere of a metal atom but also to estimate the energy of intermolecular interactions in a crystal.

This work was supported by the Russian Science Foundation (project no. 18-13-00356). The X-ray study was carried out using an equipment of the Analytical Center of the G. A. Razuvaev Institute of Organometallic Chemistry, Russian Academy of Sciences.

Online Supplementary Materials

Supplementary data associated with this article [tables containing geometrical and topological (Table S1–S6) parameters; Figures S1–S4; cif and checkcif files and details of building the invarioms and DFT calculation] can be found in the online version at doi: 10.1016/j.mencom.2021.03.012.

References

- 1 B. Dittrich, T. Koritsánszky and P. Luger, *Angew. Chem., Int. Ed.*, 2004, **43**, 2718.
- 2 B. Dittrich, C. B. Hübschle, K. Pröpper, F. Dietrich, T. Stolper and J. J. Holstein, *Acta Crystallogr.*, 2013, **B69**, 91.

- 3 B. Dittrich and M. A. Spackman, *Acta Crystallogr.*, 2007, **A63**, 426.
- 4 R. Kalinowski, B. Dittrich, C. B. Hübschle, C. Paulmann and P. Luger, *Acta Crystallogr.*, 2007, **B63**, 753.
- 5 B. Dittrich, M. Weber, R. Kalinowski, S. Grabowski, C. B. Hübschle and P. Luger, *Acta Crystallogr.*, 2009, **B65**, 749.
- 6 M. Weber, S. Grabowski, A. Hazra, S. Naskar, S. Banerjee, N. B. Mondal and P. Luger, *Chem. – Asian J.*, 2011, **6**, 1390.
- 7 P. Luger, M. Weber, C. Hübschle and R. Tacke, *Org. Biomol. Chem.*, 2013, **11**, 2348.
- 8 J. Bacsá, M. Okello, P. Singh and V. Nair, *Acta Crystallogr.*, 2013, **C69**, 285.
- 9 Yu. V. Nelyubina, A. A. Korlyukov and K. A. Lyssenko, *RSC Adv.*, 2015, **5**, 75360.
- 10 Yu. V. Nelyubina, I. V. Ananyev, V. V. Novikov and K. A. Lyssenko, *RSC Adv.*, 2016, **6**, 91694.
- 11 Y. V. Nelyubina, A. A. Korlyukov and K. A. Lyssenko, *Chem. – Eur. J.*, 2014, **20**, 6978.
- 12 Y. V. Nelyubina and K. A. Lyssenko, *Chem. – Eur. J.*, 2015, **21**, 9733.
- 13 Y. V. Nelyubina, A. A. Korlyukov, K. A. Lyssenko and I. V. Fedyanin, *Inorg. Chem.*, 2017, **56**, 4688.
- 14 C. M. Wandtke, M. Weil, J. Simpson and B. Dittrich, *Acta Crystallogr.*, 2017, **B73**, 794.
- 15 B. Dittrich, C. M. Wandtke, A. Meents, K. Pröpper, K. C. Mondal, P. P. Samuel, N. Amin, A. P. Singh, H. W. Roesky and N. Sidhu, *ChemPhysChem*, 2015, **16**, 412.
- 16 M. Malischewski, K. Seppelt, J. Sutter, F. W. Heinemann, B. Dittrich and K. Meyer, *Angew. Chem., Int. Ed.*, 2017, **56**, 13372.
- 17 B. Dittrich, E. Ruf and T. Meller, *Struct. Chem.*, 2017, **28**, 1333.
- 18 G. K. Fukin, E. V. Baranov, A. V. Cherkasov, R. V. Rummyantsev, A. N. Artemov and E. V. Sazonova, *Russ. J. Coord. Chem.*, 2019, **45**, 680 (*Koord. Khim.*, 2019, **45**, 584).
- 19 G. K. Fukin, A. V. Cherkasov, E. V. Baranov, R. V. Rummyantsev, E. V. Sazonova and A. N. Artemov, *ChemistrySelect*, 2019, **4**, 10976.
- 20 G. K. Fukin, E. V. Baranov, A. V. Cherkasov, R. V. Rummyantsev, E. A. Kozlova, L. S. Okhlopko and A. I. Poddel'sky, *Russ. Chem. Bull., Int. Ed.*, 2019, **68**, 1650 (*Izv. Akad. Nauk, Ser. Khim.*, 2019, 1650).
- 21 L. Chęcinska, S. Mebs, C. B. Hübschle, D. Förster, W. Morgenroth and P. Luger, *Org. Biomol. Chem.*, 2006, **4**, 3242.
- 22 R. Dovesi, A. Erba, R. Orlando, C. M. Zicovich-Wilson, B. Civalleri, L. Maschio, M. Rerat, S. Casassa, J. Baima, S. Salustro and B. Kirtman, *WIREs Comput. Mol. Sci.*, 2018, **8**, e1360.
- 23 E. Espinosa, E. Molins and C. Lecomte, *Chem. Phys. Lett.*, 1998, **285**, 170.
- 24 K. A. Lyssenko, A. A. Korlyukov, D. G. Golovanov, S. Yu. Ketkov and M. Yu. Antipin, *J. Phys. Chem. A*, 2006, **110**, 6545.
- 25 I. V. Glukhov, K. A. Lyssenko, A. A. Korlyukov and M. Yu. Antipin, *Russ. Chem. Bull., Int. Ed.*, 2005, **54**, 547 (*Izv. Akad. Nauk, Ser. Khim.*, 2005, 541).
- 26 P. M. Dominiak, E. Espinosa and J. Angyán, in *Modern Charge Density Analysis*, eds. C. Gatti and P. Macchi, Springer, Heidelberg, 2012, pp. 387–433.
- 27 I. V. Glukhov, K. A. Lyssenko, A. A. Korlyukov and M. Yu. Antipin, *Faraday Discuss.*, 2007, **135**, 203.
- 28 A. N. Artemov, E. V. Sazonova, N. A. Krylova, E. A. Zvereva, N. A. Pechen, G. K. Fukin, A. V. Cherkasov, V. I. Faerman and N. Yu. Grishina, *Russ. Chem. Bull., Int. Ed.*, 2018, **67**, 884 (*Izv. Akad. Nauk, Ser. Khim.*, 2018, 884).
- 29 G. M. Sheldrick, *Acta Crystallogr.*, 2015, **C71**, 3.
- 30 G. M. Sheldrick, *SADABS-2012/1*, Bruker/Siemens Area Detector Absorption Correction Program, Bruker AXS, Madison, WI, 2012.
- 31 N. K. Hansen and P. Coppens, *Acta Crystallogr.*, 1978, **A34**, 909.
- 32 C. Jelsch, B. Guillot, A. Lagoutte and C. Lecomte, *J. Appl. Crystallogr.*, 2005, **38**, 38.
- 33 F. H. Allen, O. Kennard, D. G. Watson, L. Brammer, A. G. Orpen and R. Taylor, *J. Chem. Soc., Perkin Trans. 2*, 1987, S1.
- 34 F. L. Hirshfeld, *Acta Crystallogr.*, 1976, **A32**, 239.
- 35 A. Stash and V. Tsirelson, *J. Appl. Crystallogr.*, 2002, **35**, 371.
- 36 G. K. Fukin, A. V. Cherkasov, N. Yu. Zarovkina and A. N. Artemov, *ChemistrySelect*, 2016, **1**, 5014.
- 37 L. J. Farrugia, C. Evans, D. Lentz and M. Roemer, *J. Am. Chem. Soc.*, 2009, **131**, 1251.
- 38 G. K. Fukin, A. V. Cherkasov, R. V. Rummyantsev, N. Yu. Grishina, E. V. Sazonova, A. N. Artemov and A. I. Stash, *Mendeleev Commun.*, 2019, **29**, 346.
- 39 C. A. Morrison and M. M. Siddick, *Chem. – Eur. J.*, 2003, **9**, 628.
- 40 C. A. Morrison and M. M. Siddick, *Angew. Chem., Int. Ed.*, 2004, **43**, 4780.

Received: 19th October 2020; Com. 20/6342